Tu P5 15

Dimensional Tensor Invariants in Geoelectric Prospecting

S. Szalai* (Geodetic and Geophysical Research Institute of HAS), A. Novák (MTA CSFKI GGI, POB 5, H-9401 Sopron, Hungary), M. Varga (KBFI Triász LtD, Budapest), A. Frigy (West-Hungarian University, Sopron, Hungary), M. Metwaly (King Saud University, Saudi Arabia), K. Szokoli (MTA CSFKI GGI, POB 5, H-9401 Sopron, Hungary) & L. Szarka (MTA Titkárság, Kutatóintézeti Főosztály, Budapest)

SUMMARY

It is studied whether the one-dimensional (1D), two-dimensional (2D) and three-dimensional (3D) tensor invariants really behave like invariants in the field that is whether their values are independent from the position of the current electrodes of the tensorial geoelectric configuration and what kind of results they can produce in numerical modelling and in field situations. It was shown that: 1. the invariants are “less and less” invariants with their increasing dimension number depending more and more on the position of the current electrodes. 2. They produced smaller and smaller anomalies both in their size and amplitude making the detection and interpretation of the anomalies more and more difficult. 3a. The 1D image produced for all models stable, reliable results which are ideal for creating a starting model. 3b. In spite of the uncertainty of the 2D data they improved the quality of the fault field image which has been received using the 1D data only. In the sites with building remnants and furnace however the 2D invariant was not able to give extra information to that obtained by the 1D invariant. 3c. Although the interpretation of the 3D results may be rather complicated it proved to be more useful than that of the 2D data both in the building remnants and furnace field studies. In special cases the 3D invariant may refine the 1D image. In summary the 2D invariant which is sensible to the two-dimensional changes of the subsurface (like that of the in the field practice most often used 2D ERT configuration) and which was expected to produce the best results proved to be almost the less useful in these investigations in spite of that the investigated models were more 2D/3D than 1D. Because even for such models the 1D invariant produced the best results its application is recommended. Regarding however that the 2D and 3D invariants may refine the 1D image even if their results are more uncertain joint interpretation of all dimensional invariants could also be worthwhile. Although the refined model is more risky it can be very useful e.g. in studies where the danger factor is high, e.g. because of filtrating of dangerous fluid or fissuring on the wall of a nuclear waste deposit. In such cases it is better to warn redundantly than eventually not recognize real danger. The results of these investigations should be taken into account in every research area, where tensorial measurements could be carried out, e.g. in magnetotelluric research.

Introduction

For a long time in geoelectric research profiling and soundings were carried out to measure the horizontal and the vertical changes in electric resistivity. Sometimes azimuthal measurements were applied to know the direction of structures (recently Szalai *et al.* 2009). Today ERT, especially two-dimensional (2D) ERT measurements are dominant which unify profiling and sounding, but they require the knowledge of the structure direction to get correct results. If the structure is more difficult 3D measurements or tensorial measurements are required. The tensorial measurements, which are discussed in this paper, are not dependent on the direction of the configuration. Such measurements have been carried out e.g. by Mousatov et al. (2002) and Mauriello and Patella (1999). Varga et al. (2008) studied the Pilisszentkereszt area using tensorial measurements, from where we are going to present results. While the one-dimensional (1D) invariants are sensible to the vertical changes of resistivity, the two-dimensional (2D) invariants present the best long inhomogeneities and the three-dimensional (3D) invariants describe inhomogeneities which are finite in all directions.
Due to the success of tensorial measurements and because they could also be done e.g. in magnetotellurics (e.g. Marti *et al.* 2004) or magnetic measurements (Munschy and Fleury, 2011), we wanted to investigate them more detailed. We studied the applicability of the different dimension invariants in numerical and field investigations and whether the invariants really behave like invariants even among field conditions.

Theory

On the horizontal surface the apparent resistivity tensor $\underline{\underline{\rho}}$ relates the horizontal electric field **E** and the current density vector **j** by Ohm's differential law (Bibby, 1977):

$$\mathbf{E} = \underline{\underline{\rho}}\,\mathbf{j}, \text{ that is } \begin{bmatrix} E_x \\ E_y \end{bmatrix} = \begin{bmatrix} \rho_{xx} & \rho_{xy} \\ \rho_{yx} & \rho_{yy} \end{bmatrix} \begin{bmatrix} j_x \\ j_y \end{bmatrix} \tag{1}$$

The determination of the elements of tensor $\underline{\underline{\rho}}$ is described in Bibby (1986). In order to be able to determine all elements of the resistivity tensor and therefore to be able to apply its rotational invariants at least two current directions are needed. It is possible to define an infinite number of alternative sets of three independent rotational invariants. In the simplest, mathematical approach of the DC resistivity tensor, the corresponding resistivity definitions are applied:

$$\rho_{\text{det}} = (\det \underline{\underline{\rho}})^{1/2} = (\rho_{xx}\rho_{yy} - \rho_{xy}\rho_{yx})^{1/2} \tag{2a}$$

$$\rho_{\text{ssq}} = (\tfrac{1}{2}\,\text{ssq}\,\underline{\underline{\rho}})^{1/2} = [\tfrac{1}{2}(\rho_{xx}^2 + \rho_{xy}^2 + \rho_{yx}^2 + \rho_{yy}^2)]^{1/2} \tag{2b}$$

$$\rho_{\text{trace}} = \tfrac{1}{2}(\text{trace}\,\underline{\underline{\rho}}) = \tfrac{1}{2}(\rho_{xx} + \rho_{yy}) \tag{2c}$$

Of course, any other independent invariants could be alternatively used. The set of the WAL invariants in magnetotellurics (Weaver et al. 2000), provides not only a 1D resistivity estimation, but also a 2D- and a 3D indicator about the subsurface. Instead of the seven WAL invariants in magnetotellurics (I_1-I_7), in the DC resistivity tensor only I_1, I_3 and I_5 exist. They are as follows:
1. The 1D indicator which corresponds to I_1.

$$\rho_{I_1} = \sqrt{\frac{\rho_{\text{ssq}}^2 + \rho_{\text{det}}^2}{2}} \tag{3}$$

2. The two-dimensional anisotropy, I_{2D}, obtained from the magnetotelluric parameter I_3 as

$$I_{2D} = \sqrt{\frac{\text{ssq}\,\underline{\underline{\rho}} - 2\det\underline{\underline{\rho}}}{\text{ssq}\,\underline{\underline{\rho}} + 2\det\underline{\underline{\rho}}}}\,. \tag{4}$$

3. The measure of the three-dimensionality, I_{3D}, corresponding to the original I_5:

$$I_{3D} = \frac{\rho_{xy} - \rho_{yx}}{2\Pi_2} \tag{5}$$

I_{2D} and I_{3D} are dimensionless numbers, with absolute values between 0 and 1. Any of the ρ_{det}, ρ_{ssq}, ρ_{trace} and ρ_{I_1} maps give information about the vertical changes of the resistivity. The multidimensional indicators provide additional information: I_{2D} about the sides (i.e. the "strike directions") and I_{3D} about the corners.

Field realization

One part of the field measurements were carried out in the Cistercian Monastery in Pilisszentkereszt (30 km N of Budapest, Hungary). The other part of the field measurements have been carried out in the Amphitheatre in Sopron, in Western Hungary.

In the computer-controlled measuring process the current electrodes are fixed 15 m apart and the potential electrodes are connected by multicore cables. In Figure 1 the basic field layout is shown denoted by number 1. All ΔU_x and ΔU_x potential differences are determined: at first due to current electrodes A_1B_1, then due to A_2B_2, as follows. Thus both components of the horizontal electric field vector were determined at the same instant. The current density vector values are calculated simply from the current intensity.

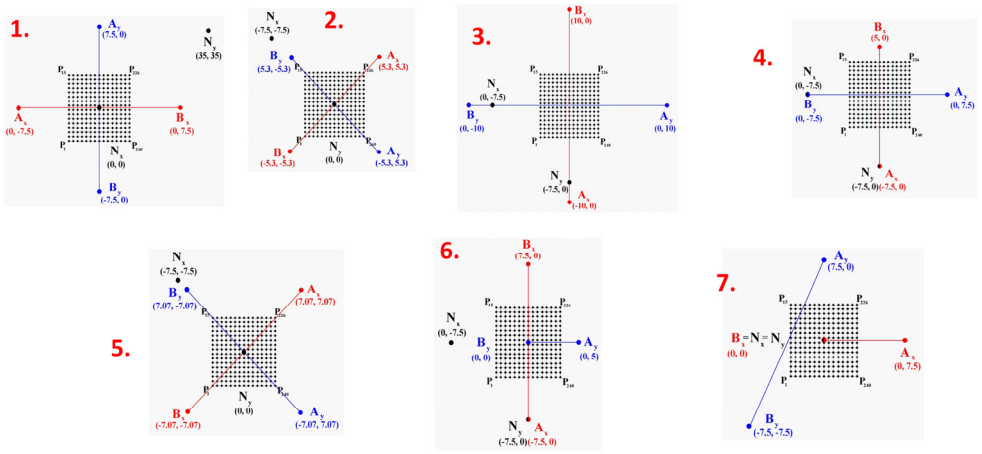

Figure 1 *Layout of the tensor measuring system. Current (A and B), reference (N) and potential electrode (P) positions of the applied configurations. The centre coordinate (0, 0) is in the focus of the area covered by the potential electrodes (P_1-P_{240}).*

In the field the current electrode distance was fixed at 15 m; two perpendicular AB directions were used, and 16·15=240 potential electrodes (with an equidistant space of 50 cm in both x and y directions) were put in the central (nearly square, 7.5m · 7m) area between the current electrodes.

Results and conclusions

Geoelectric numerical modelling and field measurements have been carried out for various models to see the usefulness of various dimensional tensor invariants.

Summarising the results of the numerical and field investigations over the wall remnants and the furnace (Figs. 2, 3), it can be stated that: 1) the 1D invariants are very robust, and are hardly influenced by the noise. Their image is very convincing, ideal for the first step of the interpretation which may even be the final step. 2) In these models in field the 2D invariant could not give additional information compared to the one obtained by any 1D invariant. The interpretation of the 2D images is rather difficult (furnace) or the image cannot be interpreted at all (wall remnants). 3) Although the interpretation of the 3D result may be very difficult (with the exception if parts of the inhomogeneity extend not parallel to the coordinate axes) its results may be better than those of the 2D invariant. It does not seem to give additional information beyond the one obtained from any 1D measurement or at least the validity of the information is questionable. 4) On the basis of the above considerations, the interpretation of the results of any 1D invariant is recommended which could eventually be completed by results from the 3D invariant.

The joint interpretation of the 1D and 2D images obtained over a fault verified that this fault is not linear and that there is a remarkable horst in the bedrock surface whose effect was earlier believed to

be noise on the base of the 1D image. The joint interpretation of the 1D and 2D results improved the quality of the interpretation. The 3D invariant could not further improve it although there have to be 3D effects attached to the variations of the bedrock relief. The linear structures in the 3D image are believed to be artificial on basis of the numerical results and the small size anomalies would not give considerable supplementary information even if they would eventually be valid.

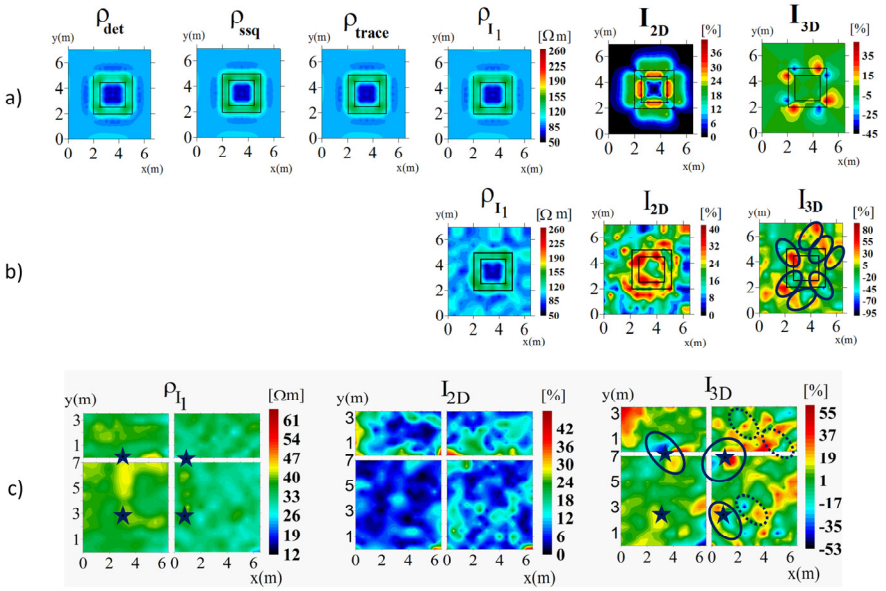

Figure 2 *Numerical results over the wall remnant model. a) model with the first set of independent invariants (ρ_{det}, ρ_{ssq}, ρ_{trace}) and the DC versions of the WAL invariants (ρ_{I_1}, I_{2D} and I_{3D}). b) model with the WAL invariants. Data contaminated with 3% Gaussian noise. Host resistivity: 100 ohmm; parameters of the walls: their resistivity is 1000 ohmm, burial depth is 0 m and thickness is 0.5 m.* ***c)*** *Field results with WAL invariants over the wall remnant model. Stars denote the positions of the corners on the basis of the 1D image. The continuous-line ellipses enclose the more characteristic, the dotted-line ellipses the less characteristic anomaly pairs.*

To see how far the given invariants really behave like invariants, field investigation has been carried out over a fault using different layouts (Fig. 1). The 1D and 2D images which were obtained using different current electrode distances (Fig. 4) are hardly different from each other. If the direction of the lines of the current electrode pairs were different in the investigated configurations, there were significant differences especially among the 2D images.

The 1D invariant proved to be the less sensitive to the position of the current electrodes. Since the 1D images are very similar for each configuration, the application of one 1D invariant is sufficient. We prefer to apply the WAL invariant like for the 2D and 3D invariants. In the field, the 2D invariant barely behaved like an invariant, while the 3D invariant seemed to be not at all invariant.

As already mentioned, the 3D invariant was not able to improve the 1D+2D image. Although many 3D anomalies are supposed to be linked to the curve of the fault, their position is also the function of the given configuration. Because there are a lot of uncertainties according to the reality of the 3D anomalies, it would be useful to study the usefulness of the 3D invariant e.g. by physical modelling.

Acknowledgements

J. Túri and Zs. Pap took part in the field measurement or/and the data processing. S. Szalai, one of the authors of this paper is a grantee of the Bolyai János Scholarship.

References

Bibby H.M. [1977] The apparent resistivity tensor. *Geophysics,* **42**, 1258-1261.

Bibby H.M. [1986] Analysis of multiple-source bipole-quadripole resistivity surveys using the apparent resistivity tensor. *Geophysics,* **51**, 972-983.

Marti A., Queralt, P., Roca, E., [2004] Geoelectric dimensionality in complex geologic areas: application to the Spanish Betic Chain. *Geophysical Journal International,* **157**, 961-974.

Mauriello P. and Patella D. [1999] Resistivity imaging by probability tomography. *Geophysical Prospecting,* **47**, 411-429.

Mousatov, A., Pervago, E., Shevnin V. [2002] Anisotropy Determination In Heterogeneous Media By Tensor Measurements of the Electric Field, 2002 *SEG Annual Meeting*, SEG-2002-1444.

Munschy M. Fleury S. [2011] Scalar, vector, tensor magnetic anomalies: measurement or computation? *Geophysical Prospecting,* 2011, **59**, 1035-1045.

Szalai, S., Kósa, I., Nagy, T., Szarka, L., [2009] Effectivity enhancement of azimuthal geoelectric measurements in determination of multiple directions of subsurface fissures, on basis of analogue modelling experiments, *15th European Meeting of Environmental and Engineering Geophysics*, 25-28.

Szarka L. [1987] Geophysical mapping by stationary electric and magnetic field components: a combination of potential gradient mapping and magnetometric resistivity (MMR) methods. *Geophysical Prospecting,* **35**, 424-444.

Varga, M., Novák, A., Szarka, L. [2008] Application of tensorial electrical resistivity mapping to archaeological prospection, *Near-Surface Geophysics,* **6**, 39-47.

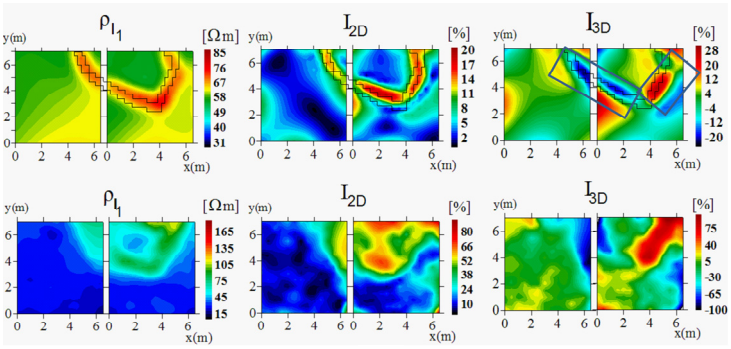

Figure 3 *The DC versions of the WAL invariants (ρ_{I_1}, I_{2D} and I_{3D}) over the furnace model. First row: modelling results in presence of ±3% random noise, added to the electric field. Resistivity of the host rock: 30 Ω m. Resistivity, depth, thickness of the wall and the vertical elongation of the furnace are 3000 Ω m, 0.5 m, 0.5 m and 1 m, respectively. Second row: Field results with the same invariants.*

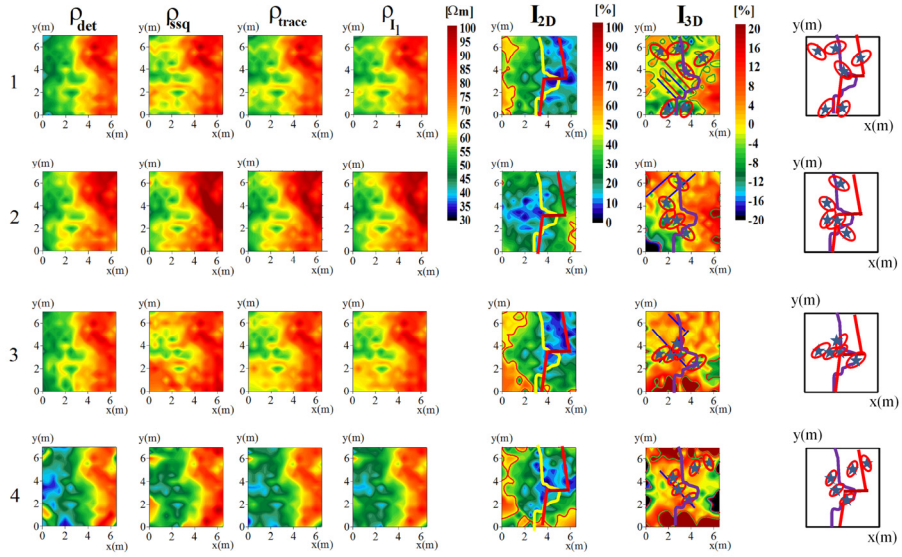

Figure 4 *Many of the results of the field study carried out by different configurations. The mathematical invariants (ρ_{det}, ρ_{ssq}, ρ_{trace}) and the WAL invariants (ρ_{I_1}, I_{2D} and I_{3D}) are shown. Last column: the interpretation of the I_{3D} map. The curve presents the supposed line of the fault on the basis of the 1D image of configuration 5, while the red lines follow the small value zone in the 2D image on the basis of the image of the same configuration. The ellipses delineate small-size 3D anomalies. The stars present the position of the supposed 3D inhomogeneities.*